Theory of resonant Brillouin scattering in population-inverted semiconductors. II. Expressions of photoelastic constants in zinc-blende semiconductors and numerical examples

Masamichi Yamanishi
Department of Physical Electronics, Faculty of Engineering, Hiroshima University, Sendamachi 3-8-2, Hiroshima, 730 Japan

Nobuo Mikoshiba
Research Institute of Electrical Communication, Tohoku University, Katahira 2-1-1, Sendai, 980 Japan

Tadatsugu Minami
Department of Electrical Engineering, Kanazawa Institute of Technology, Ōgigaoka 7-1, Nonoichi, Ishikawa, 921 Japan

(Received 10 August 1979)

Explicit expressions for the photoelastic constants in zinc-blende semiconductors are given based on the general expressions obtained in a previous paper. Numerical examples for unexcited and population-inverted GaAs are given by taking account of (i) the existence of the imaginary part overlooked so far, (ii) the enhancement of the hydrostatic deformation potential due to the carrier-carrier interaction, (iii) the contribution from the free-carrier plasma screening and absorption due to intraband transitions, and (iv) the nondispersive contribution from the higher bands. In relation to the existence of the imaginary part, we propose a possible explanation of the dispersion of the photoelastic constant observed by Garrod and Bray, which has not been clearly explained. We predict a new effect that the scattered photon intensity can be larger than the incident photon intensity even if the photons are absorbed, when the intensity of acoustical phonons is sufficiently large.

I. INTRODUCTION

We have developed a general theory of photoelastic constants in population-inverted semiconductors by solving the equation of motion for one-particle density matrix in the preceding paper.[1] In this paper, we derive the explicit expressions of photoelastic constants in zinc-blende crystals based on the general expressions and present numerical examples for GaAs.

In Sec. II, we derive the explicit expressions of photoelastic constants in zinc-blende crystals, taking account of the effects of interband and intraband transitions. In Sec. III, we present the numerical examples of the dispersion curves of the photoelastic constants for unexcited and population-inverted GaAs. The importance of the imaginary part of the photoelastic constant and a new effect caused by the existence of such an imaginary part are discussed in some detail. Moreover, we propose a possible explanation of the experimental results on the dispersion of the photoelastic constants p_{44} of GaAs by Garrod and Bray,[2] which could not have been clearly explained so far, by taking account of the effect of the imaginary part. In Appendix A, the expressions of deformation potentials and momentum matrix elements in zinc-blende crystals are derived. In Appendix B, we discuss a possibility of enhancement of the hydrostatic deformation potential in population-inverted semiconductors and give an estimate of the magnitude of the enhanced deformation potential.

II. PHOTOELASTIC CONSTANTS IN ZINC-BLENDE SEMICONDUCTORS

We must designate a specific crystal structure in order to calculate explicitly photoelastic constants by making use of Eq. (21) in the previous paper.[1] Let us consider a zinc-blende crystal with direct gap, such as GaAs, InP, and their mixed compounds, etc. As shown in Fig. 1, the band structure consists of one s-like conduction band and three p-like valence bands. The three valence bands are named heavy hole band, light hole band, and spin-orbit split-off band, respectively. In what follows, we use the subscripts V_h, V_l, and V_s for the quantities related to the heavy hole band, the light hole band, and the spin-orbit split-off band, respectively. The energy in the conduction band is given by

$$\epsilon_C(\vec{k}) = \hbar^2 k^2/2m_C + \epsilon_C \quad . \tag{1}$$

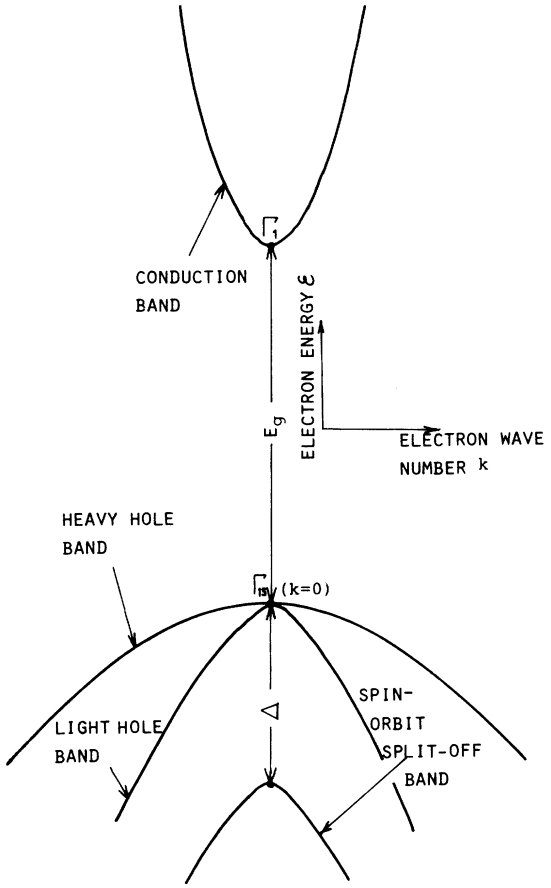

FIG. 1. Illustration of energy-band diagram of a zinc-blende semiconductor considered in this paper.

The energies in the valence bands are given by

$$\epsilon_{V_h}(\vec{k}) = \epsilon_{V_h} - \hbar^2 k^2/2m_{V_h} \ ,$$
$$\epsilon_{V_l}(\vec{k}) = \epsilon_{V_l} - \hbar^2 k^2/2m_{V_l} \ , \qquad (2)$$
$$\epsilon_{V_s}(\vec{k}) = \epsilon_{V_s} - \hbar^2 k^2/2m_{V_s} \ .$$

The following relations between the band-edge energies exist:

$$\epsilon_C - \epsilon_{V_h} = E_g \ ,$$
$$\epsilon_{V_h} = \epsilon_{V_l} \ , \qquad (3)$$
$$\epsilon_{V_h} - \epsilon_{V_s} = \Delta \ ,$$

where E_g and Δ are the energy gap and the spin-orbit splitting energy, respectively.

The eigenfunctions of the conduction and valence bands are given by

$$|C, \vec{k}\rangle = |e^{i\vec{k}\cdot\vec{r}} u_C\rangle \ , \quad |V_h, \vec{k}\rangle = |e^{i\vec{k}\cdot\vec{r}} u_{V_h}\rangle \ ,$$
$$|V_l, \vec{k}\rangle = |e^{i\vec{k}\cdot\vec{r}} u_{V_l}\rangle \ , \quad |V_s, \vec{k}\rangle = |e^{i\vec{k}\cdot\vec{r}} u_{V_s}\rangle \ ,$$

where $|u_C\rangle$, $|u_{V_h}\rangle$, $|u_{V_l}\rangle$, and $|u_{V_s}\rangle$ are the periodic functions. $|u_C\rangle$ is an s-like isotropic function, while $|u_{V_l}\rangle$ $(l = h, l, s)$ is a p-like function. So, we must take care of the relation between the direction of applied stress due to phonons and the quantization axis of the p-like functions, since zinc-blende crystals are isotropic under unstressed conditions and an anisotropy is induced by applying the stress to the crystal. On the calculations of piezobirefringence and stress-induced electroreflectance coefficients, Pollak, Cardona, and Higginbotham[3,4] chose the quantization axis parallel to the applied static stress. Following their idea on the selection of the quantization axis, we calculate the photoelastic constants p_{11}, p_{12}, and p_{44} in zinc-blende crystals.

A. Photoelastic constants p_{11} and p_{12}

Let us consider a longitudinal sound wave, propagating along the [001] axis of a zinc-blende crystal. Nonzero components of stress and strain tensors associated with the wave are T_{33} and S_{33}, respectively. Therefore, the quantization axis should be parallel to the [001] axis. Then, the wave functions of the conduction and valence bands in the (J,m_J) representation are given by[3,5]

$$|u_C\rangle = |S\uparrow\rangle \ \text{ or } \ |S\downarrow\rangle \ ,$$

$$|u_{V_h}\rangle = |\tfrac{3}{2},\tfrac{1}{2}\rangle_{001} = (\tfrac{1}{6})^{1/2}|2Z\uparrow - (X+iY)\downarrow\rangle$$

or

$$= |\tfrac{3}{2},-\tfrac{1}{2}\rangle_{001} = (\tfrac{1}{6})^{1/2}|2Z\downarrow - (X-iY)\uparrow\rangle \ ,$$

$$|u_{V_l}\rangle = |\tfrac{3}{2},\tfrac{3}{2}\rangle_{001} = (\tfrac{1}{2})^{1/2}|(X+iY)\uparrow\rangle$$

or (4)

$$= |\tfrac{3}{2},-\tfrac{3}{2}\rangle_{001} = (\tfrac{1}{2})^{1/2}|(X-iY)\downarrow\rangle \ ,$$

$$|u_{V_s}\rangle = |\tfrac{1}{2},\tfrac{1}{2}\rangle_{001} = (\tfrac{1}{3})^{1/2}|Z\uparrow + (X+iY)\downarrow\rangle$$

or

$$= |\tfrac{1}{2},-\tfrac{1}{2}\rangle_{001} = (\tfrac{1}{3})^{1/2}|Z\downarrow + (X-iY)\uparrow\rangle \ ,$$

where $\uparrow$ and $\downarrow$ indicate spin up and spin down referring to the [001] axis. $|S\rangle$ is the s-like wave function and $|X\rangle$, $|Y\rangle$, and $|Z\rangle$ are the p-like wave functions whose forms are given in Appendix A.

The orbital-strain Hamiltonian H_{xv} is written[6]

$$H_{xv} = -a(S_{11}+S_{22}+S_{33})$$
$$-3b[(L_1^2 - \tfrac{1}{3}L^2)S_{11} + \text{c.p.}]$$
$$-(6d/\sqrt{3})(\{L_1L_2\}S_{12} + \text{c.p.}) \ , \qquad (5)$$

where L is the angular momentum operator, c.p. denotes cyclic permutations with respect to the in-

dices 1, 2, and 3, and the quantities in the curly brackets indicate the symmetrical product, $\{L_1L_2\}=\frac{1}{2}(L_1L_2+L_2L_1)$. Parameter a is the hydrostatic-pressure deformation potential for a given band which is defined as the difference between the hydrostatic-pressure deformation potentials for the conduction and valence bands. The parameters b and d are uniaxial deformation potentials of the valence bands. For the longitudinal wave propagating along the [001] axis, the orbital-strain Hamiltonian H_{xv} becomes

$$H_{xv}=-aS_{33}-3b[(L_3^2-\tfrac{1}{3}L^2)S_{33}] \quad . \tag{6}$$

From Eqs. (4) and (6), the Hamiltonian matrix for the valence bands can be written (see Appendix A)

$$\begin{array}{c} \left|\frac{3}{2},\pm\frac{1}{2}\right\rangle_{001} \quad \left|\frac{3}{2},\pm\frac{3}{2}\right\rangle_{001} \quad \left|\frac{1}{2},\pm\frac{1}{2}\right\rangle_{001} \\ \left\|\begin{array}{ccc} (-a+b)S_{33} & 0 & \sqrt{2}bS_{33} \\ 0 & -(a+b)S_{33} & 0 \\ \sqrt{2}bS_{33} & 0 & -aS_{33} \end{array}\right\| \end{array} \quad . \tag{7}$$

Therefore, nonzero components of the deformation potentials are given by

$$\begin{aligned} &e(C_{33}^{(CC)}-C_{33}^{(V_hV_h)})=|e|(a-b) \quad , \\ &e(C_{33}^{(CC)}-C_{33}^{(V_lV_l)})=|e|(a+b) \quad , \\ &e(C_{33}^{(CC)}-C_{33}^{(V_sV_s)})=|e|a \quad , \\ &eC_{33}^{(V_hV_s)}=|e|\sqrt{2}b \quad , \end{aligned} \tag{8}$$

where a and b are given in eV.

The momentum matrix elements are written (see Appendix A)

$$\begin{aligned} &|M_{CV_h}|_{\parallel}^2=2|M|^2 \quad , \\ &|M_{CV_l}|_{\parallel}^2=0 \quad , \\ &|M_{CV_s}|_{\parallel}^2=|M|^2 \quad , \\ &(M_{CV_h}M_{V_sC})_{\parallel}=\sqrt{2}|M|^2 \end{aligned} \tag{9}$$

and

$$\begin{aligned} &|M_{CV_h}|_{\perp}^2=\tfrac{1}{2}|M|^2 \quad , \\ &|M_{CV_l}|_{\perp}^2=\tfrac{3}{2}|M|^2 \quad , \\ &|M_{CV_s}|_{\perp}^2=|M|^2 \quad , \\ &(M_{CV_h}M_{V_sC})_{\perp}=-(1/\sqrt{2})|M|^2 \quad , \end{aligned} \tag{10}$$

where subscripts $\parallel$ and $\perp$ denote the components of the momentum matrix elements parallel and perpendicular to the [001] axis, respectively. $|M|^2$ is the square of the absolute value of the matrix elements averaged with respect to directions and is given by[7]

$$|M|^2=\tfrac{1}{6}m_0E_g(m_0/m_C-1)(E_g+\Delta)/(E_g+\tfrac{2}{3}\Delta) \quad . \tag{11}$$

Inserting Eqs. (8) and (9) into Eq. (21) of the previous paper,[1] we obtain the explicit expression of the photoelastic constant $\Delta p_{11}=\Delta p_{22}=\Delta p_{33}\equiv\Delta p_{33,33}$:

$$\begin{aligned} \Delta p_{11}=\frac{1}{2}\left(\frac{e}{m_0}\right)^2\frac{|e||M|^2}{\pi^2\omega^2\epsilon_0 n^4}\Bigg[&(a-b)\left(\int_0^\infty\frac{\partial f_C(k)/\partial\epsilon_C+\partial f_{V_h}(k)/\partial\epsilon_{V_h}}{\epsilon_C(k)-\epsilon_{V_h}(k)-\hbar\omega-i\hbar/\tau_{CV_h}}k^2dk-2\int_0^\infty\frac{[f_C(k)-f_{V_h}(k)]k^2dk}{[\epsilon_C(k)-\epsilon_{V_h}(k)-\hbar\omega-i\hbar/\tau_{CV_h}]^2}\right) \\ &+\frac{a}{2}\left(\int_0^\infty\frac{(\partial f_C(k)/\partial\epsilon_C)k^2dk}{\epsilon_C(k)-\epsilon_{V_s}(k)-\hbar\omega-i\hbar/\tau_{CV_s}}-2\int_0^\infty\frac{[f_C(k)-f_{V_s}(k)]k^2dk}{[\epsilon_C(k)-\epsilon_{V_s}(k)-\hbar\omega-i\hbar/\tau_{CV_s}]^2}\right) \\ &+4b\int_0^\infty\frac{[f_C(k)-f_{V_h}(k)]k^2dk}{[\epsilon_C(k)-\epsilon_{V_h}(k)-\hbar\omega-i\hbar/\tau_{CV_h}][\epsilon_C(k)-\epsilon_{V_s}(k)-\hbar\omega-i\hbar/\tau_{CV_s}]}\Bigg] \quad . \end{aligned} \tag{12}$$

From Eq. (21) of the previous paper,[1] with Eqs. (8) and (10), the photoelastic constant $\Delta p_{12}=\Delta p_{13}=\Delta p_{23}=\Delta p_{22,33}$ can be written

$$\begin{aligned} \Delta p_{12}=\frac{1}{2}\left(\frac{e}{m_0}\right)^2\frac{|e||M|^2}{\pi^2\omega^2\epsilon_0 n^4}\Bigg[&\tfrac{1}{4}(a-b)\left(\int_0^\infty\frac{[\partial f_C(k)/\partial\epsilon_C+\partial f_{V_h}(k)/\partial\epsilon_{V_h}]k^2dk}{\epsilon_C(k)-\epsilon_{V_h}(k)-\hbar\omega-i\hbar/\tau_{CV_h}}-2\int_0^\infty\frac{[f_C(k)-f_{V_h}(k)]k^2dk}{[\epsilon_C(k)-\epsilon_{V_h}(k)-\hbar\omega-i\hbar/\tau_{CV_h}]^2}\right) \\ &+\tfrac{3}{4}(a+b)\left(\int_0^\infty\frac{[\partial f_C(k)/\partial\epsilon_C]k^2dk}{\epsilon_C(k)-\epsilon_{V_l}(k)-\hbar\omega-i\hbar/\tau_{CV_l}}-2\int_0^\infty\frac{[f_C(k)-f_{V_l}(k)]k^2dk}{[\epsilon_C(k)-\epsilon_{V_l}(k)-\hbar\omega-i\hbar/\tau_{CV_l}]^2}\right) \\ &+\frac{a}{2}\left(\int_0^\infty\frac{[\partial f_C(k)/\partial\epsilon_C]k^2dk}{\epsilon_C(k)-\epsilon_{V_s}(k)-\hbar\omega-i\hbar/\tau_{CV_s}}-2\int_0^\infty\frac{[f_C(k)-f_{V_s}(k)]k^2dk}{[\epsilon_C(k)-\epsilon_{V_s}(k)-\hbar\omega-i\hbar/\tau_{CV_s}]^2}\right) \\ &-2b\int_0^\infty\frac{[f_C(k)-f_{V_h}(k)]k^2dk}{[\epsilon_C(k)-\epsilon_{V_h}(k)-\hbar\omega-i\hbar/\tau_{CV_h}][\epsilon_C(k)-\epsilon_{V_s}(k)-\hbar\omega-i\hbar/\tau_{CV_s}]}\Bigg] \quad , \end{aligned} \tag{13}$$

where n is the isotropic refractive index of the zinc-blende crystal. In the derivation, we used the following approximations:

$$\epsilon_{V_h}(k)-\epsilon_{V_s}(k)-\hbar\Omega-i\hbar/\tau_{V_hV_S}\simeq\epsilon_{V_h}(k)-\epsilon_{V_s}(k)\ ,$$

$$\epsilon_{V_h}(k)-\epsilon_{V_s}(k)+i\hbar/\tau_{CV_h}-i\hbar/\tau_{CV_s}\simeq\epsilon_{V_h}(k)-\epsilon_{V_s}(k)\ , \tag{14}$$

which are valid for III-V compounds. Although the valence band V_1 degenerates to the valence band V_h at $k=0$, almost all the holes occupy the band V_h because of $m_{V_h} >> m_{V_l}$. Therefore, we can take the band V_h as the highest valence band V_1 in Eq. (21) of the previous paper.[1]

B. Photoelastic constants p_{44}

Photoelastic constant p_{44} is defined as the change of dielectric constant ϵ_{12} for a strain S_{12}. The strain S_{12} is given by

$$S_{12}=\frac{1}{2}\left(\frac{\partial u_x}{\partial y}+\frac{\partial u_y}{\partial x}\right)\ ,$$

where u_x and u_y are the x and y components of the displacement associated with a shear wave propagated along the [001] axis of zinc-blende crystals. In this case, we should take the z axis, i.e., the [001] axis as a special direction, so that the wave functions of Eq. (4) referred to the [001] axis can be used in the calculation of p_{44}.

From Eq. (5), the orbital-strain Hamiltonian H_{xv} becomes

$$H_{xv}=-\sqrt{3}d(L_1L_2+L_2L_1)S_{12}\ . \tag{15}$$

By using Eq. (15) and Eqs. (A1), (A2), and (A3) in Appendix A, we obtain nonzero components of the Hamiltonian matrix

$$\begin{aligned}
C_{12}^{(V_hV_l)}&=\langle\tfrac{3}{2},\pm\tfrac{1}{2}|H_{xv}|\tfrac{3}{2},\mp\tfrac{3}{2}\rangle=\pm id\ ,\\
C_{12}^{(V_lV_h)}&=\langle\tfrac{3}{2},\pm\tfrac{3}{2}|H_{xv}|\tfrac{3}{2},\mp\tfrac{1}{2}\rangle=\pm id\ ,\\
C_{12}^{(V_sV_l)}&=\langle\tfrac{1}{2},\pm\tfrac{1}{2}|H_{xv}|\tfrac{3}{2},\mp\tfrac{3}{2}\rangle=\mp\sqrt{2}id\ ,\\
C_{12}^{(V_lV_s)}&=\langle\tfrac{3}{2},\pm\tfrac{3}{2}|H_{xv}|\tfrac{1}{2},\mp\tfrac{1}{2}\rangle=\mp\sqrt{2}id\ .
\end{aligned} \tag{16}$$

The matrix elements related to the intraband transitions with spin reversals have finite value, but the momentum matrix elements related to the transitions becomes zero. Therefore, no intraband transition contributes to the photoelastic constant p_{44}.

Nonzero components of momentum matrix elements can be written (see Appendix A)

$$\begin{aligned}
(M_{CV_h})_1(M_{V_lC})_2&=\langle S\uparrow\text{ or }\downarrow|P_x|\tfrac{3}{2},\pm\tfrac{1}{2}\rangle\\
&\quad\times\langle\tfrac{3}{2},\mp\tfrac{3}{2}|P_y|S\downarrow\text{ or }\uparrow\rangle\\
&=\mp i\tfrac{1}{2}\sqrt{3}M^2\ ,\\
(M_{CV_l})_1(M_{V_hC})_2&=\langle S\downarrow\text{ or }\uparrow|P_x|\tfrac{3}{2},\mp\tfrac{3}{2}\rangle\\
&\quad\times\langle\tfrac{3}{2},\pm\tfrac{1}{2}|P_y|S\downarrow\text{ or }\uparrow\rangle\\
&=\pm i\tfrac{1}{2}\sqrt{3}M^2\ ,\\
(M_{CV_s})_1(M_{V_lC})_2&=\langle S\downarrow\text{ or }\uparrow|P_x|\tfrac{1}{2},\pm\tfrac{1}{2}\rangle\\
&\quad\times\langle\tfrac{3}{2},\mp\tfrac{3}{2}|P_y|S\downarrow\text{ or }\uparrow\rangle\\
&=\pm i(\tfrac{3}{2})^{1/2}M^2\ ,\\
(M_{CV_l})_1(M_{V_sC})_2&=\langle S\downarrow\text{ or }\uparrow|P_x|\tfrac{3}{2},\mp\tfrac{3}{2}\rangle\\
&\quad\times\langle\tfrac{1}{2},\pm\tfrac{1}{2}|P_y|S\downarrow\text{ or }\uparrow\rangle\\
&=\mp i(\tfrac{3}{2})^{1/2}M^2\ .
\end{aligned} \tag{17}$$

Inserting Eqs. (16) and (17) with the approximation [Eq. (14)] into Eq. (21) of the previous paper,[1] we obtain the explicit expression of the photoelastic constant Δp_{44}:

$$\begin{aligned}
\Delta p_{44}=\frac{\sqrt{3}}{4}\left(\frac{e}{m_0}\right)^2\frac{|e||M|^2d}{\pi^2\omega^2\epsilon_0n^4}\Bigg(&-\int_0^\infty\frac{[f_{V_h}(k)-f_{V_l}(k)]k^2dk}{[\epsilon_C(k)-\epsilon_{V_l}(k)-\hbar\omega-i\hbar/\tau_{CV_l}][\epsilon_{V_h}(k)-\epsilon_{V_l}(k)-\hbar\Omega-i\hbar/\tau_{V_hV_l}]}\\
&-\int_0^\infty\frac{[f_{V_l}(k)-f_{V_h}(k)]k^2dk}{[\epsilon_C(k)-\epsilon_{V_h}(k)-\hbar\omega-i\hbar/\tau_{CV_h}][\epsilon_{V_l}(k)-\epsilon_{V_h}(k)-\hbar\Omega-i\hbar/\tau_{V_lV_h}]}\\
&+\int_0^\infty\frac{[2f_C(k)-f_{V_h}(k)-f_{V_l}(k)]k^2dk}{[\epsilon_C(k)-\epsilon_{V_h}(k)-\hbar\omega-i\hbar/\tau_{CV_h}][\epsilon_C(k)-\epsilon_{V_l}(k)-\hbar\omega-i\hbar/\tau_{CV_l}]}\\
&+4\int_0^\infty\frac{[f_C(k)-f_{V_l}(k)]k^2dk}{[\epsilon_C(k)-\epsilon_{V_l}(k)-\hbar\omega-i\hbar/\tau_{CV_l}][\epsilon_C(k)-\epsilon_{V_s}(k)-\hbar\omega-i\hbar/\tau_{CV_s}]}\Bigg)\ .
\end{aligned} \tag{18}$$

Thus, we obtained the explicit expressions [Eqs. (12), (13), and (18)] for the contribution from the interband transitions between the conduction and valence bands to three independent photoelastic constants p_{11}, p_{12}, and p_{44} in zinc-blende semiconductors, taking account of the effects of population inversion and of intraband relaxation. Here, let us consider some effects which are not taken into account in our theory.

The first effect is the renormalization of the band-gap energy due to the carrier-carrier interaction. As discussed in Appendix B, the fluctuation of the electron density, induced by low frequency phonons, in population-inverted semiconductors brings about the additional change of the band gap through the carrier-carrier interaction, i.e., the change of exchange energy. As a result, the hydrostatic deformation potential is enhanced as follows:

$$a^* = [(2-A)/(2-2A)]a \quad , \tag{19}$$

where the constant A is given by

$$A = \frac{1}{3}\left(\frac{|e|}{2\pi\epsilon_0\epsilon_r}\right)\left(\frac{3}{\pi}\right)^{1/3} n_C^{-2/3}\frac{\partial n_C}{\partial \epsilon_C} \quad . \tag{20}$$

In this expression, ϵ_r and n_C are the specific dielectric constant and the conduction-electron density, respectively. For example, in the case of a population-inverted GaAs at room temperature, the electron density n_C is of the order of 10^{18} cm^{-3},[8] so that the constant A becomes about 0.85. Then, the hydrostatic deformation potential is strongly enhanced; i.e., $a^* = 3.8a$. On the calculation of the photoelastic constants p_{11} and p_{12} in the population-inverted semiconductor, we must use the enhanced value a^* for the hydrostatic deformation potential a.

The second is the effects of the intraband transitions due to the photons. The effects are well known as free-carrier plasma screening and free-carrier absorption. The changes of refractive index due to the former process and of absorption coefficient due to the latter process are given by[9,10]

$$\begin{aligned} \Delta n &= -e^2\lambda_0^2 n_C/8\pi^2\epsilon_0 n m_C c^2 \quad , \\ \Delta\alpha &= e^2\lambda_0^2 n_C/8\pi^2\epsilon_0 n m_C c^3 \tau_C \quad , \end{aligned} \tag{21}$$

respectively, where λ_0 and c are the wavelength of incident and scattered photons and the light velocity in vacuum, respectively. Similar expressions can be written for holes, but the effects due to the holes can be neglected because of $m_{V_h} >> m_C$. When a longitudinal sound wave propagates along the [001] axis in the population-inverted zinc-blende semiconductor, the electron density n_C is modulated through the enhanced deformation potential a^* by the sound wave. Therefore, the above processes contribute to the photoelastic constants p_{11} and p_{12}. From the definition of photoelastic constants and Eq. (21), we can obtain the expressions for the contribution from the intraband transitions due to the photons to the photoelastic constants

$$\begin{aligned} \Delta p'_{11} = \Delta p'_{12} &= -\frac{2}{n^3}\left[\frac{\partial \Delta n}{\partial n_C} - i\left(\frac{\lambda_0}{2\pi n}\right)\frac{\partial \Delta\alpha}{\partial n_C}\right]\frac{\partial n_C}{\partial \epsilon_C}\frac{a^*}{2} \\ &= -\frac{e^2\lambda_0^2}{4\pi^2\epsilon_0 n^4 m_C c^2}\left(1 - \frac{i\lambda_0}{2\pi n c\tau_C}\right)\frac{\partial n_C}{\partial \epsilon_C}\frac{a^*}{2} \quad . \end{aligned} \tag{22}$$

The third effect is the contribution to the photoelastic constants p_{11}, p_{12}, and p_{44} from higher bands ($M_1, M_2, \ldots$ critical points) which are relatively nondispersive in the energy range of the photons considered in this paper and unaffected by the population change of carriers. Here, the contributions from the higher bands are dealt with as fitting parameters $\Delta p''_{ij}$. We adjust the fitting parameters in such a way that the calculated values of the photoelastic constants agree with the measured values at the low energy range of the photons.

III. NUMERICAL EXAMPLES AND DISCUSSION

Here we show the numerical examples of the photoelastic constants for GaAs calculated based on Eqs. (12), (13), (18), and (22). Before carrying out the numerical calculations, we check the values of the refractive index n which should be used in the equations. The refractive index has a weak dispersion as a function of the photon energy and has an imaginary part which corresponds to the absorption (or amplification) coefficient. However, the dispersion and imaginary part can be neglected in the calculations of the photoelastic constants. For example, in the case of GaAs, the refractive index changes by only 4.4% (Ref. 11) when the photon energy changes from 1.2 to 1.45 eV. The absorption coefficient for the photon energy above the band gap is of the order of 10^4 cm^{-1},[12] which corresponds to the imaginary part of the refractive index of about 4×10^{-2}, much smaller than the real part of 3.6.

The numerical values for various physical quantities used in the numerical calculations are listed up in Table I. In the numerical calculations of Δp_{ij} in Eqs. (12), (13), and (18), the integrations were carried out numerically with the help of a digital computer. For convenience, we write down the expression for the contribution $\Delta p'_{11} = \Delta p'_{12}$ to the photoelastic constants from the intraband transitions in a numerical form for population-inverted GaAs:

$$\begin{aligned} \Delta p'_{11} = \Delta p'_{12} &= 0.1(1.41/h\nu)^2 \\ &\times [1 - i2.6\times10^{-4}(1.41/h\nu)] \quad , \end{aligned} \tag{22'}$$

TABLE I. Numerical values for physical quantities in GaAs.

$E_g = 1.41$ eV[a]	$a = -8.9$ eV[b]
$\Delta = 0.34$ eV[c]	$b = -4.1$ eV[d]
$m_C = 0.066 m_0$[e]	$d = -5.4$ eV[f]
$m_{V_h} = 0.5 m_0$[g]	$a^* = 4a = -35.6$ eV
$m_{V_l} = 0.09 m_0$[g]	$\Delta p_{11}'' = -0.154$[h]
$m_{V_s} = 0.15 m_0$[i]	$\Delta p_{12}'' = -0.073$[h]
$\tau_{CV_h} = \tau_{CV_l} = \tau_{CV_s} = \tau_{V_h V_l} = 5\times10^{-13}$ sec[j]	$\Delta p_{44}'' = -0.122$[h]
$n = 3.6$[k]	

[a]Reference 12.
[b]R. N. Bargave and M. I. Nathan, Phys. Rev. 161, 695 (1967).
[c]M. Cardona, K. L. Shaklee, and F. H. Pollak, Phys. Rev. 154, 696 (1967).
[d]P. Y. Yu, M. Cardona, and F. H. Pollak, Phys. Rev. B 3, 340 (1971).
[e]Q. H. F. Vrehen, J. Phys. Chem. Solids 29, 129 (1968).
[f]A. Gavini and M. Cardona, Phys. Rev. B 1, 672 (1970).
[g]A. K. Walton and U. K. Mishra, Proc. Phys. Soc. London 1, 533 (1968).
[h]Values are adjusted in such a way that the calculated values of p_{ij} agree with the measured values at the low-energy range of the photons.
[i]O. V. Emelyanenko, Phys. Status Solidi 8, K155 (1965).
[j]This value was used in the analysis of GaAs lasers [see, M. Yamada and Y. Suematsu, Proceedings of the Tenth Conference on Solid State Devices, 1978 [Jpn. J. Appl. Phys. Suppl. 18-1, 347 (1979)].
[k]D. T. F. Marple, J. Appl. Phys. 35, 1241 (1964).

where we express $h\nu$ in eV and assume the electron density n_C of 10^{18} cm^{-3}, which is a typical value in a GaAs laser at room temperature.[8] The real part of $\Delta p_{11}'$ (or $\Delta p_{12}'$) can contribute significantly to the photoelastic constant p_{11} (or p_{12}), while the imaginary parts of them are negligibly small over the energy range of the photons considered in this paper. In the cases of unexcitation, the photoelastic constants p_{ij} are given by the sum of Δp_{ij} and $\Delta p_{ij}''$, while in the cases of population inversion, the photoelastic constants p_{ij} are given by the sum of Δp_{ij}, $\Delta p_{ij}'$, and $\Delta p_{ij}''$.

Strictly speaking, in population-inverted semiconductors, the band gap E_g is renormalized by the carrier-carrier interaction as discussed in Appendix B, so that we must use the renormalized value $E_g^* = E_g - \Delta E_g$ as the band gap. The band-gap contraction ΔE_g calculated with the help of Eq. (B1) in Appendix B is of the order of a few tens of meV. However, in the reported values for the energy gap E_g of GaAs, there is the uncertainty of the same orders of magnitude as the band-gap contraction ΔE_g. Therefore, we used the bare value E_g as the band-gap energy even in the case of population inversion.

We show the calculated values of the photoelastic constants p_{11}, p_{12}, and p_{44} as a function of the photon energy in Figs. 2, 3, and 4, respectively. As shown in Fig. 2(a), there exists a weak resonant enhance-

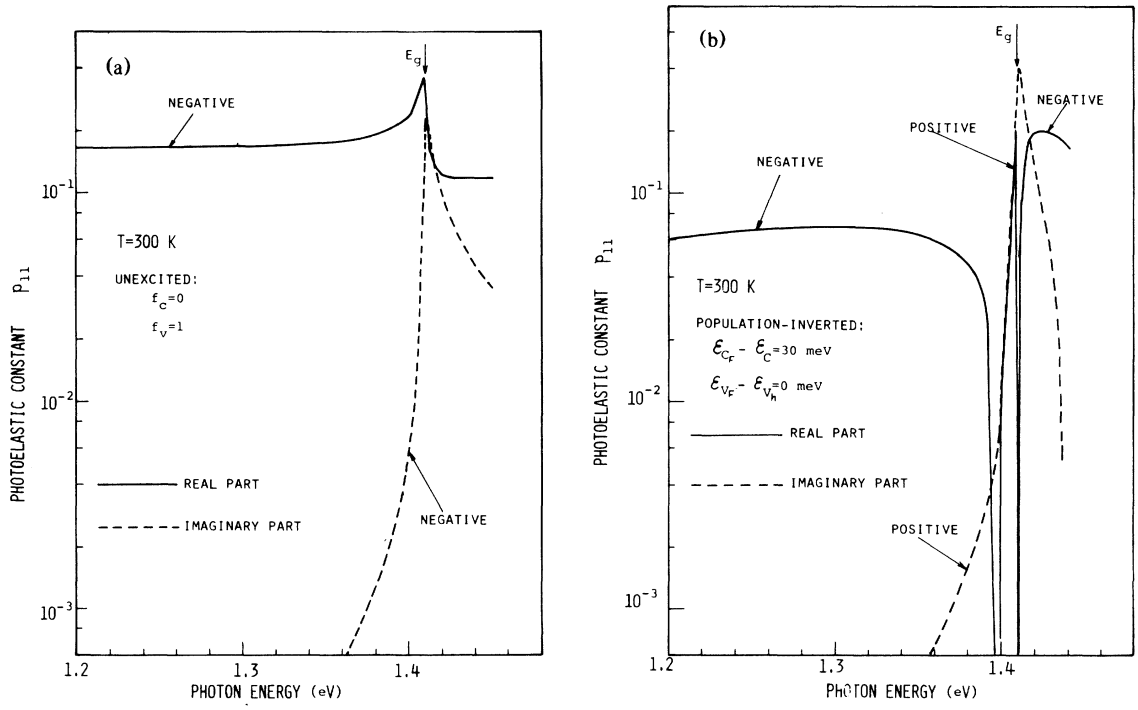

FIG. 2. Calculated photoelastic constant p_{11} as a function of photon energy at room temperature in (a) unexcited and (b) population-inverted GaAs. The values of quasi-Fermi levels, i.e., $\epsilon_{C_F} - \epsilon_C = 30$ meV and $\epsilon_{V_F} - \epsilon_{V_h} = 0$ meV, assumed in the cases of population inversion through Figs. 2 to 4, are typical values in a GaAlAs-GaAs heterostructure laser. We assumed the common quasi-Fermi level ϵ_{V_F} for three valence bands.

ment in the real part of the photoelastic constant p_{11} under unexcitation, since the contribution Δp_{11} from the interband transitions has the same sign (negative) as the contribution $\Delta p_{11}''$ from the higher bands. The imaginary part of the photoelastic constant p_{11} cannot be neglected near the band gap E_g. In the case of population inversion, the dispersion of the photoelastic constant p_{11} shown in Fig. 2(b) has the following characteristic features: (i) there exist two cancellation points, i.e., 1.398 and 1.410 eV in the real-part dispersion curves and (ii) the imaginary part has the opposite sign (positive) to the imaginary part of p_{11} in the case of unexcitation. On the electronic transition from the energy level $\epsilon_V(k)$ to $\epsilon_C(k)$ or vise versa in population-inverted semiconductors, the factor $(f_C - f_V)$ in the resonant terms of Eq. (12) can take a positive value if $\epsilon_C(k) - \epsilon_V(k) < \epsilon_{C_F} - \epsilon_{V_F}$, in contrast to the case of unexcitation, while the factor $(f_C - f_V)$ takes a negative value if $\epsilon_C(k) - \epsilon_V(k) > \epsilon_{C_F} - \epsilon_{V_F}$ even in the case of population inversion. Therefore, the electronic transitions where $\epsilon_C(k) - \epsilon_V(k) < \epsilon_{C_F} - \epsilon_{V_F}$ contribute with a positive sign to the photoelastic constant p_{11}. This is the reason for the appearance of the cancellations of the real part of p_{11} and the sign reversal of the imaginary part, associated with the population inversion. Here, we check numerically the magnitude of the other contributions to the photoelastic constant p_{11}. One is the contribution to the photoelastic constant directly induced by electron-density fluctuation due to phonons, which corresponds to the terms involving $\partial f_C/\partial \epsilon_C$ or $\partial f_V/\partial \epsilon_V$ in Eq. (12). Both real and imaginary parts of the sum of the terms take positive values which are of the same orders of magnitude as the sum of the resonant terms over the entire energy range. Another is the contribution of the intraband transitions to the photoelastic constant. As one can see in Eq. (22'), the intraband contribution $\Delta p_{11}'$ take large positive values, i.e., ~ 0.1. Therefore, we must take into account of the both effects of the electron-density fluctuation and intraband transitions. Finally, it should be noted that the imaginary part of p_{11} in the case of population inversion is quite dominant near the band gap.

The dispersion-curves of the photoelastic constant p_{12} in the cases of unexcitation and population inversion, shown in Figs. 3(a) and 3(b), have features similar to those of the photoelastic constant p_{11}. The appearance of the cancellations of the real part and the sign-reversal of the imaginary part, associated with the population inversion, are due to the same reason as that in the photoelastic constant p_{11}. In this case, the electron-density fluctuation and the intraband transitions make also significant contribution to the photoelastic constant p_{12}.

As shown in Fig. 4(a), the cancellation of the real part of the photoelastic constant p_{44} occurs at 1.4 eV in the case of unexcited GaAs but the scattering cross section never becomes zero at the cancellation point because of the existence of the imaginary part

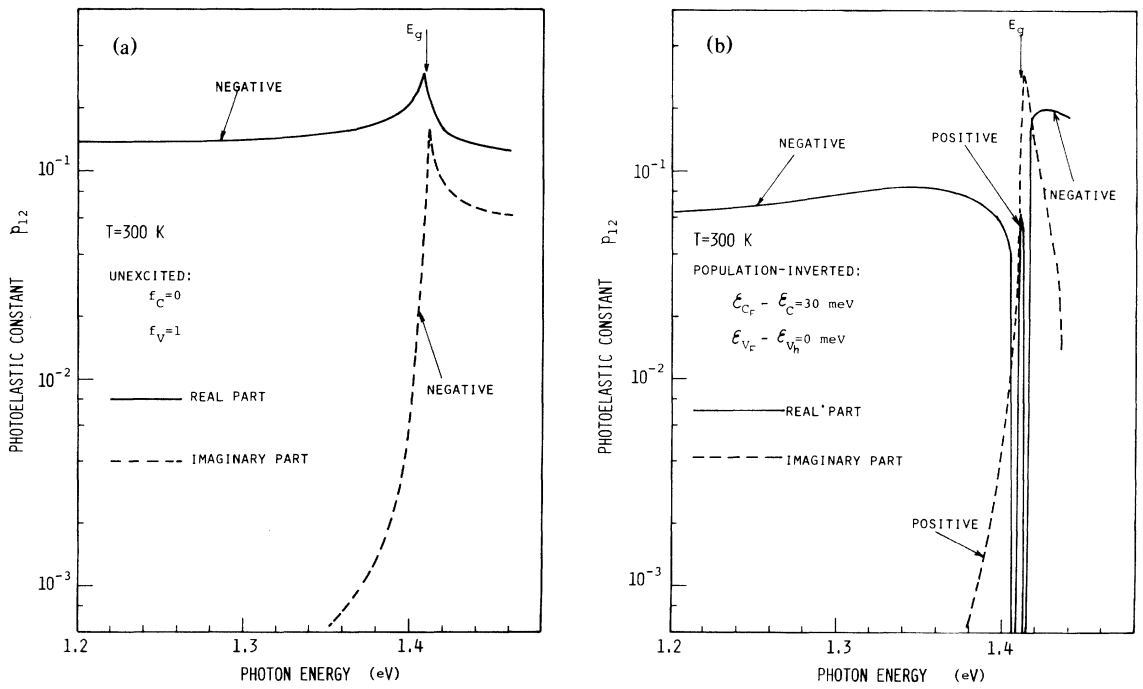

FIG. 3. Calculated photoelastic constant p_{12} as a function of photon energy at room temperature in (a) unexcited and (b) population-inverted GaAs.

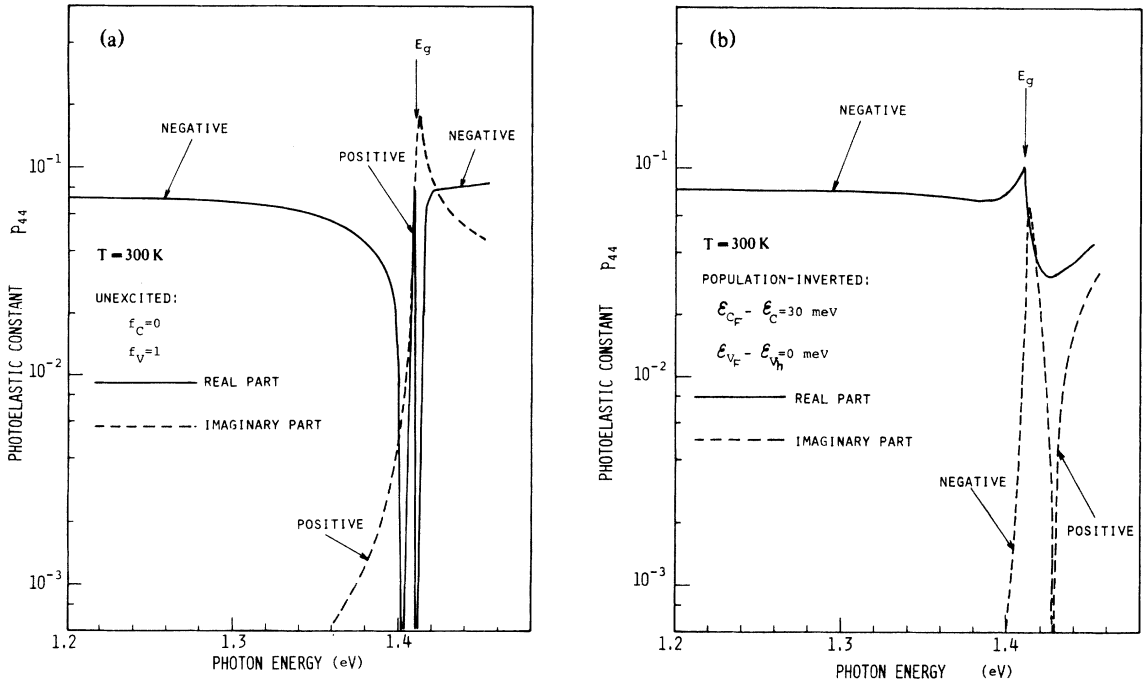

FIG. 4. Calculated photoelastic constant p_{44} as a function of photon energy at room temperature in (a) unexcited and (b) population-inverted GaAs.

of p_{44} at the point. More detailed discussion on this subject will be made later. Near the energy gap, the imaginary part of p_{44} in the case of unexcitation is also quite important. In contrast to the case of unexcitation, there exists a very weak resonance in the real part of p_{44} in population-inverted GaAs, as shown in Fig. 4(b).

Let us discuss in more detail the importance of the imaginary part of photoelastic constant near the band gap overlooked so far, and discuss some new effects caused by the existence of such an imaginary part. Also, in relation to the existence of the imaginary part, our calculated result on p_{44} in the case of unexcitation is compared with the experimental results by Garrod and Bray,[2] which have not yet been clearly explained so far. As is well known, the scattering efficiency in Brillouin scattering (Bragg regime) is given by[13]

$$I_s/I_0 = |\sin(\omega ln^3 pS/2c)|^2 e^{-\alpha l/\cos\theta} , \quad (23)$$

where I_0 and I_s are the intensities of the incident and scattered photons, respectively. Also, l and θ are the beam width of the phonons and the incident (or scattered) angle in the crystal, respectively. The subscripts of the photoelastic constant p and the strain S are dropped and the photoelastic constant can be regarded as a complex number, i.e., $p = p_r + ip_i$. The refractive index n can be regarded as a pure real number, as discussed in the first paragraph of this section.

In the small-signal case; $|\omega ln^3 pS/2c| \ll 1$, Eq. (23) can be rewritten approximately in the form

$$I_s/I_0 = e^{-\alpha l/\cos\theta} \omega^2 l^2 n^6 S^2 |p|^2/4c^2 . \quad (24)$$

In this case, the scattering efficiency I_s/I_0, i.e., the scattering cross section is proportional to the square of the absolute value of the complex photoelastic constant p. Therefore, if we take into account of the imaginary part of the photoelastic constant, the scattering cross section should not approach zero even at the photon energy where a complete cancellation of the real part of the photoelastic constant occurs. Garrod and Bray[2] found experimentally that there exists a finite minimum in the dispersion curve of the Brillouin-scattering cross section in an unexcited GaAs and that the depth of the minimum is decreased as the phonon intensity increases. Neither of the phenomena has yet been explained clearly. The former phenomenon can be explained straightforwardly by taking into account of the imaginary part of the photoelastic constant. The latter also can be explained by the existence of the imaginary part as follows. The photoelastic constant can be regarded as a pure imaginary number near the minimum in the dispersion curve because the real part is completely cancelled out at the minimum. In such a case, the scattering cross section is proportional to the square of the sinh function

$$\sigma_{Bi} \propto e^{-\alpha l/\cos\theta} \sinh^2(\omega ln^3 p_i S/2c) .$$

On the other hand, in the region such as low-energy side of the minimum, where the photoelastic constant can be regarded as a pure real number, the scattering cross section is proportional to the square of the sinusoidal function

$$\sigma_{Br} \propto e^{-\alpha l/\cos\theta} \sin^2(\omega \ln^3 p_r S/2c) \ .$$

The scattering cross section σ_{Bi} increases more rapidly than the scattering cross section σ_{Br}, as the phonon intensity S increases. This means that the depth of the minimum in the dispersion curves of the scattering cross section is decreased with the increase of the phonon intensity.

Finally, we predict a very interesting effect caused by the existence of the imaginary part of the photoelastic constant. When the photoelastic constant is regarded as a pure real number, the sinusoidal function is smaller than unity. Therefore, as is well known, I_s is smaller than I_0 so far as the semiconductor has no gain for the incident and scattered photons. On the other hand, in the case where the photoelastic constant is a complex number, I_s can be larger than I_0 even if the photons are absorbed. For example, if we assume a pure imaginary photoelastic constant, the scattering efficiency is written as follows:

$$I_s/I_0 = e^{-\alpha l/\cos\theta} \sinh^2(\omega \ln^3 p_i S/2c) \ . \tag{25}$$

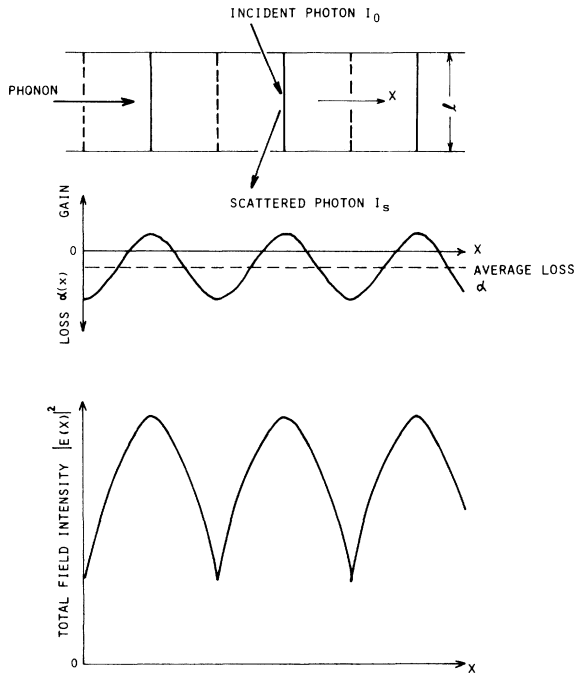

FIG. 5. Schematic drawing of the distribution of the total field intensity, associated with the incident and scattered photons, in the Bragg scattering where the loss modulation $\alpha(x)$ due to the phonons plays a main role.

that is, the scattering efficiency I_s/I_0 can be larger than unity for the sufficiently intense phonon flux. This theoretical result can be explained as follows. The effective absorption constant for the total field of the incident and scattered photons is proportional to:

$$\int \alpha(x)|E(x)|^2 dx \ ,$$

where $\alpha(x)$ is the loss modulation and $E(x)$ is the total field which consists of the sum of the incident and scattered photon fields. As is shown in Fig. 5, the total field distribution has its maximum in the minimum loss points and minimum in the maximum ones so that the effective absorption constant can be smaller than the average loss α. Also, as an extreme case, if the amplitude of the phonon is sufficiently large, one can expect a gain for the photons even if the semiconductor has an average loss. The similar explanation has been proposed by Yariv and Yeh,[14] concerning an x-ray laser oscillation in distributed feedback cavities where artificial periodic loss modulations are assumed.

IV. CONCLUSION

We have derived the explicit expressions of photoelastic constants due to the interband transitions in zinc-blende crystals based on the general theory developed in the previous paper.[1] The numerical examples were given on the dispersion curves of the photoelastic constants for GaAs, taking account of the effects of the intraband transitions, the nondispersive contribution from higher bands, and the enhancement of the hydrostatic deformation potential due to the carrier-carrier interaction in addition to the effects of the interband transitions. We have shown numerically the importance of the imaginary part of the photoelastic constant, over looked so far, in both cases of unexcitation and population inversion. In relation to the existence of such an imaginary part, we have proposed a possible explanation of the dispersion of the photoelastic constant by Garrod and Bray,[2] which has not been clearly explained. Also, we have predicted a very interesting effect that the scattered photon intensity can be larger than the incident photon intensity, even if the photons are absorbed, when the photoelastic constant has a finite imaginary part.

ACKNOWLEDGMENTS

We wish to express our thanks to K. Tsubouchi and K. Wasa for their helpful discussions. This work was partially supported by Scientific Research Grant-In-Aid (Special Research Project: Optical Guided Wave Electronics) from the Ministry of Education,

Japan, by the Research Grant from the Mitsubishi Foundation and by an RCA Research Grant.

APPENDIX A: DERIVATIONS OF DEFORMATION POTENTIALS AND MOMENTUM MATRIX ELEMENTS IN ZINC-BLENDE SEMICONDUCTORS

The wave functions of p-like valence bands in Eq. (4) are given by[4,5]

$$\left(\frac{-1}{\sqrt{2}}\right)|X+iY\rangle=\begin{bmatrix}1\\0\\0\end{bmatrix}, \quad \left(\frac{-1}{\sqrt{2}}\right)|X-iY\rangle=\begin{bmatrix}0\\0\\1\end{bmatrix}, \quad |Z\rangle=\begin{bmatrix}0\\1\\0\end{bmatrix} \tag{A1}$$

in the representation of angular-momentum operator

$$L_x=\frac{1}{\sqrt{2}}\begin{bmatrix}0&1&0\\1&0&1\\0&1&0\end{bmatrix}, \quad L_y=\frac{1}{\sqrt{2}}\begin{bmatrix}0&-i&0\\i&0&-i\\0&i&0\end{bmatrix}, \quad L_z=\begin{bmatrix}1&0&0\\0&0&0\\0&0&-1\end{bmatrix}. \tag{A2}$$

Using Eqs. (A1) and (A2) with the relations for spins

$$\langle\uparrow|\uparrow\rangle=\langle\downarrow|\downarrow\rangle=1, \quad \langle\uparrow|\downarrow\rangle=\langle\downarrow|\uparrow\rangle=0, \tag{A3}$$

we can easily obtain Eqs. (7) and (16) in the text.

From the symmetry consideration, nonzero components of the momentum matrix elements are given by[4,5]

$$P=\langle X\uparrow|P_x|S\uparrow\rangle=\langle Y\uparrow|P_y|S\uparrow\rangle=\langle Z\uparrow|P_z|S\uparrow\rangle, \tag{A4}$$

and similar equations can be written for spin-down functions. Using Eq. (A4), we can easily obtain Eqs. (9), (10), and (17) in the text.

APPENDIX B: ENHANCEMENT OF DEFORMATION POTENTIALS DUE TO CARRIER-CARRIER INTERACTION

When a semiconductor is so highly excited as to be population inverted, the band-gap energy of the semiconductor is renormalized by the many-body effect due to the excited high-density electrons. The renormalization of the band gap, i.e., the shrinkage of the conduction band edge in semiconductor lasers has been found experimentally by many researchers.[15–18] The amount of the shrinkage has been explained by considering exchange energy due to the electrons which is given by[19]

$$E_{ex}=-(|e|/2\pi\epsilon_0\epsilon_r)(3/\pi)^{1/3}n_C^{1/3}, \tag{B1}$$

where ϵ_r and n_C are the specific dielectric constant of the semiconductor and the electron density, respectively. The exchange energy due to the holes can be neglected, since the effective masses of the holes in III-V compounds are much larger than those of the electrons and then the correlation parameter r_s of the holes are larger than unity.

When a low-frequency longitudinal sound wave propagates along the [001] direction in the zinc-blende semiconductor, the band gap of the semiconductor is modulated by the sound wave, as shown by the solid lines in Fig. 6. Simultaneously, the electrons and holes are accumulated at the minimum points of the band gap and conversely depleted at the maximum points of the band gap. In the small-signal case, the ac component of the electron density, induced by the low-frequency phonons, is given by

$$\Delta n_C=\frac{\partial n_C}{\partial\epsilon_C}\frac{e(C_{ij}^{(CC)}-C_{ij}^{(V_hV_h)})S_{ij}}{2}, \tag{B2}$$

where $\frac{1}{2}e(C_{ij}^{(CC)}-C_{ij}^{(V_hV_h)})S_{ij}$ is the effective potential fluctuation for the electrons in the population-inverted semiconductors, which was discussed in Appendix A of the previous paper.[1] In the expression, the electron density n_C can be written

$$n_C=\int_0^\infty N_C(\epsilon)f_C(\epsilon,\epsilon_{C_F}-\epsilon_C)\,d\epsilon, \tag{B3}$$

where $N_C(\epsilon)$ is the density of states of the conduction band. The increase of the electron density at the minimum points of the band gap (or the decrease at the maximum points) brings about further decrease (or increase) of the band gap at the points through the change of exchange energy, as shown by the broken line in Fig. 6. From Eqs. (B1) and (B2), the ad-

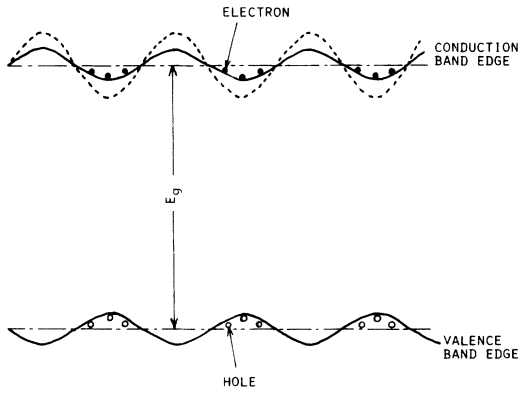

FIG. 6. Illustration of the deformation potential enhanced by the carrier-carrier interaction in a population-inverted semiconductor.

ditional change of the band gap can be written

$$\frac{\partial E_{ex}}{\partial n_C}\Delta n_C = \frac{1}{3}\left(\frac{|e|}{2\pi\epsilon_0\epsilon_r}\right)\left(\frac{3}{\pi}\right)^{1/3} \times n_C^{-2/3}\frac{\partial n_C}{\partial \epsilon_C}\frac{e(C_{ij}^{(CC)}-C_{ij}^{(V_hV_h)})S_{ij}}{2} \quad . \text{(B4)}$$

The additional change of the band gap brings about further change of the electron density. Thus, the changes of the band gap and of the electron density occurs sequentially. As a result, the total change of the band edge of the conduction band, i.e., the effective potential change for the electrons can be written as

$$e(C_{ij}^{(CC)}-C_{ij}^{(V_hV_h)})(\tfrac{1}{2}S_{ij})(1+A+A^2+\cdots) = e(C_{ij}^{(CC)}-C_{ij}^{(V_hV_h)})(\tfrac{1}{2}S_{ij})[1/(1-A)] \quad , \text{(B5)}$$

where the constant A smaller than unity is given by

$$A = \frac{1}{3}\left(\frac{|e|}{2\pi\epsilon_0\epsilon_r}\right)\left(\frac{3}{\pi}\right)^{1/3} n_C^{-2/3}\frac{\partial n_C}{\partial \epsilon_C} \quad . \text{(B6)}$$

Therefore, the fluctuation of the band gap, which is enhanced by the many-body effect, is given by

$$e(C_{ij}^{(CC)}-C_{ij}^{(V_hV_h)})(\tfrac{1}{2}S_{ij})\{[1/(1-A)]+1\} = e(C_{ij}^{(CC)}-C_{ij}^{(V_hV_h)})S_{ij}(2-A)/(2-2A) \quad .$$

Because $a >> b$, it can be regarded that the hydrostatic deformation potential a is enhanced as follows:

$$a^* = [(2-A)/(2-2A)]a \quad . \text{(B7)}$$

The uniaxial deformation potential b in fourth expression of Eq. (8) in the text is not affected by the carrier-carrier interaction, since b in the expression is related to the interband transitions between the valence bands V_h and V_s. For the same reason, d in Eq. (18) is also unaffected by the carrier-carrier interaction.

Before closing this Appendix, let us check the applicable regime of the above discussion. First, let us consider the relaxation time of the enhancement of the deformation potential. There exist two processes, i.e., one is the carrier accumulation or depletion and another is the renormalization of the band gap due to the carrier-carrier interaction. The relaxation time of the former process is smaller than 100 psec in the case of population-inverted GaAs, as discussed in Appendix A of the previous paper.[1] The relaxation time of the latter process is of the order of picosecond, which has been measured experimentally.[20] Therefore, the above discussion is valid for the phonons with the frequency lower than 10 GHz. The second is the problem on the validity of the perturbation treatment. For example, in the case of population-inverted GaAs at room temperature, a typical electron density is of the order of 10^{18} cm^{-3} and the perturbation parameter A becomes about 0.85. With respect to this problem, more exact treatment may be required. Here, we use Eq. (B7) as the expression for an order estimation.

[1]M. Yamanishi and N. Mikoshiba, preceding paper, Phys. Rev. B 21, 4763 (1980).
[2]D. K. Garrod and R. Bray, Phys. Rev. B 6, 1314 (1972).
[3]F. H. Pollak and M. Cardona, Phys. Rev. 172, 816 (1968).
[4]C. W. Higginbotham, M. Cardona, and F. H. Pollak, Phys. Rev. 184, 821 (1969).
[5]See, for example, C. Kittel, *Quantum Theory of Solids* (Wiley, New York, 1966), pp. 268–286; E. O. Kane, in *Semiconductor and Semimetal, Vol. 1, Physics of III-V Compounds*, edited by R. K. Willardson and A. C. Beer (Academic, New York, 1960), p. 75.
[6]G. E. Pikus and G. L. Bir, Sov. Phys. Solid State 1, 136 (1959); 1, 1502 (1960); G. E. Pikus, Sov. Phys. JETP 14, 1075 (1962).
[7]E. O. Kane, J. Phys. Chem. Solids 1, 249 (1959).
[8]See, for example, H. Kressel and J. K. Butler, *Semiconductor Lasers and Heterojunction LEDs* (Academic, New York, 1977), Chap. 2.
[9]Chapter 5 in Ref. 8.
[10]Chapter 8 in Ref. 8.
[11]D. D. Sell, H. C. Casey, Jr., and K. W. Wecht, J. Appl. Phys. 45, 2650 (1974).
[12]M. D. Sturge, Phys. Rev. 127, 768 (1962).
[13]See, for example, A. Yariv, *Introduction to Optical Electronics* (Holt, Reinhert, and Winston, New York, 1971), Chap. 12.
[14]A. Yariv and P. Yeh, Opt. Commun. 22, 5 (1979).
[15]N. G. Basov, O. V. Bogdankevich, V. A. Goncharov, B. M. Lavrushin, and V. Yu. Sudzilovskii, Sov. Phys. Doklady 11, 522 (1966).
[16]J. A. Rossi, D. L. Keune, N. Holonyak, Jr., D. D. Dupkus, and R. D. Bunham, J. Appl. Phys. 41, 312 (1970).
[17]H. Kressel, H. F. Lockwood, F. H. Nicoll, and M. Ettenberg, IEEE J. Quantum Electron. QE-9, 383 (1973).
[18]T. Minami, M. Yamanishi, T. Kawamura, and U. Kubo, Jpn. J. Appl. Phys. 15, 1117 (1976).
[19]P. A. Wolf, Phys. Rev. 126, 405 (1962).
[20]C. W. Shank, R. L. Fork, R. F. Leheny, and Jagdeep Shah, Phys. Rev. Lett. 42, 112 (1979).